Kinoshita et al. *Zool. Res.* 2025, 46(3): 608−617
https://doi.org/10.24272/j.issn.2095-8137.2024.343
https://cstr.cn/32248.14.zr.2024.343

ZR | Zoological Research

Article Open Access

Effects of targeted deletion of a 284 bp avian-specific highly conserved element within the *Sim1* gene on flight feather development in chickens

Keiji Kinoshita[1,2,#], Kumiko Tanabe[1,2,#], Muhammad Ameen Jamal[1,2,3], Momoko Kyu-Shin[4], Kai-Xiang Xu[1,2], Yan-Hua Su[1,2], Xiong Zhang[1,2], Takayuki Suzuki[4,*], Hong-Jiang Wei[1,2,3,*]

[1] *State Key Laboratory for Conservation and Utilization of Bio-Resources in Yunnan*, *Yunnan Agricultural University*, *Kunming*, *Yunnan* 650201, *China*

[2] *Key Laboratory for Porcine Gene Editing and Xenotransplantation in Yunnan Province*, *Yunnan Agricultural University*, *Kunming*, *Yunnan* 650210, *China*

[3] *State Key Laboratory of Genetic resources and Evolution*, *Kunming Institute of Zoology*, *Chinese Academy of Sciences*, *Kunming*, *Yunnan* 650223, *China*

[4] *Graduate School of Science*, *Department of Biology*, *Osaka Metropolitan University*, *Sumiyoshi-ku*, *Osaka* 558-8585, *Japan*

ABSTRACT

Flight feathers represent a hallmark innovation of avian evolution. Recent comparative genomic analyses identified a 284 bp avian-specific highly conserved element (ASHCE) located within the eighth intron of the SIM bHLH transcription factor 1 (*Sim1*) gene, postulated to act as a *cis*-regulatory element governing flight feather morphogenesis. To investigate its functional significance, genome-edited (GE) primordial germ cell (PGC) lines carrying targeted ASHCE deletions were generated using CRISPR/Cas9-mediated editing, with germline chimeric males subsequently mated with wild-type (WT) hens to obtain GE progeny. The resulting GE chickens harbored 257–260 bp deletions, excising approximately half of the *Sim1*-ASHCE sequence. Reverse transcription-quantitative real-time polymerase chain reaction (RT-qPCR) analysis showed an average 0.32-fold reduction in *Sim1* expression in the forelimbs of GE embryos at day 8 (E8) compared to WT counterparts. Despite this, GE chickens developed structurally normal flight and tail feathers. *In situ* hybridization localized *Sim1* expression to the posterior mesenchyme surrounding flight feather buds in E8 WT embryos, but not within the buds themselves. These results suggest that partial deletion of *Sim1*-ASHCE, despite diminishing *Sim1* expression, does not disrupt flight feather formation. The excised region appears to possess enhancer activity toward *Sim1* but is dispensable for flight feather development. Complete ablation of the ASHCE will be necessary to fully resolve the regulatory role of *Sim1* in avian feather morphogenesis.

Keywords: *Sim1* gene; Avian-specific enhancer; Flight feather development; Primordial germ cell; Genome editing

INTRODUCTION

Birds represent a pivotal lineage in vertebrate evolution, comprising over 10 000 species worldwide (Brown et al., 2003). Among these, chickens are widely regarded as a representative species and a valuable model for studying gene function and trait development (Flores-Santin & Burggren, 2021). Wings, a defining innovation of birds, enable powered flight through evolutionary adaptations such as lightweight skeletal structures, aerodynamic beak morphologies, and feathers specialized for lift generation (Lynch et al., 2018; Rayner, 1988). Feathers are essential for flight efficiency and stability. Fossil evidence suggests that wings and feathers first emerged in feathered dinosaurs, the direct ancestors of modern birds, with the discovery of four-winged basal dromaeosaurids in China further illustrating the ancient origins of flight-related traits (Brusatte et al., 2015; Xu et al., 2003).

Comparative genomic analyses have identified conserved regulatory elements critical to the development of avian traits such as flight, beak morphology, and feather architecture (Jarvis et al., 2014; Lamichhaney et al., 2015; Lopes et al.,

Received: 29 December 2024; Accepted: 15 January 2025; Online: 16 January 2025

Foundation items: This work was supported by the Ministry of Agriculture and Rural Affairs of the People's Republic of China (125A0607) and Department of Science and Technology of Yunnan Province (XDYC-KJLJ-2022-0004)

[#]Authors contributed equally to this work

*Corresponding authors, E-mail: suzuki.takayuki@omu.ac.jp; hongjiangwei@126.com

2016; Sackton et al., 2019). These non-coding regions, particularly conserved regulatory elements, are crucial for phenotypic diversity and evolutionary adaptation by precisely regulating the expression of genes in specific tissues and across various developmental stages. Sequence variation within these regions can alter gene regulatory networks, drive phenotypic diversification, and enhance environmental adaptability.

Feather development and diversity have been extensively studied, offering valuable insights into their evolutionary origins, structure, and function. Recent studies and reviews have explored the evolutionary forces shaping feather morphology (Terrill & Shultz, 2023), genetic mechanisms underpinning feather diversity (Ng & Li, 2018), genomic determinants of epidermal appendage patterning (Boer et al., 2017), and molecular processes governing feather development and regeneration (Chen et al., 2015). These findings collectively highlight the intricate relationship between genetic regulation and the evolutionary success of avian feathers.

A significant breakthrough in avian genomics was the identification of avian-specific highly conserved elements (ASHCEs), including a 284 bp enhancer associated with SIM bHLH transcription factor 1 (*Sim1*) (Seki et al., 2017). Among millions of ASHCEs, *Sim1*-ASHCE is notable for its forelimb-specific enhancer activity, homologous to bird wings, thus suggesting a specialized role in flight feather formation. Transgenic reporter assays in mice have demonstrated that this *cis*-regulatory element drives forelimb-specific gene expression, emphasizing its evolutionary significance in the emergence of flight adaptations in birds.

Sim genes, including *Sim1* and *Sim2*, encode transcription factors initially identified in *Drosophila* as regulators of cell fate during midline development (Crews, 1998; Crews & Fan, 1999). In vertebrates, *Sim1* is essential for hypothalamic development, particularly the formation of the paraventricular nucleus involved in energy balance and feeding regulation (Coumailleau & Duprez, 2009). Knockout (KO) of *Sim1* in mice results in hyperphagia, obesity, and metabolic dysregulation (Michaud et al., 2001), while mutations in human *Sim1* are associated with Prader-Willi-like syndrome, exhibiting similar metabolic disturbances (Bonnefond et al., 2013). In chickens, homologs of *Sim1* and *Sim2* contribute to hypothalamic and amygdalar development, potentially influencing reproductive behavior and neurodevelopment (Metwalli et al., 2022). Furthermore, while the specific role of *Sim1* in early embryonic development requires further investigation, its expression has been associated with limb morphogenesis in both chick and mouse models (Coumailleau & Duprez, 2009), suggesting involvement in critical physiological processes. Despite these established roles, the function of *Sim1* in avian flight feather formation, particularly through the 284 bp ASHCE, has yet to be explored.

The advent of CRISPR/Cas9 genome editing has revolutionized functional genetic research across multiple taxa, including birds (Lee et al., 2020; Popova et al., 2023). Although avian genome editing initially faced challenges due to the unique developmental environment of birds (Khwatenge & Nahashon, 2021), advances in primordial germ cell (PGC) culture methods have enabled more stable cultivation and germline transmission through chimeric birds (Whyte et al., 2015). Genome editing technologies such as TALENs and CRISPR/Cas9 have enabled precise genetic modifications, including KO and knock-in (KI) chickens, advancing functional interrogation of avian genomes (Ballantyne et al., 2021; Jiang et al., 2020; Kinoshita et al., 2024; Oishi et al., 2018; Park et al., 2014).

In this study, CRISPR/Cas9 was used to target the 284 bp avian-specific enhancer *Sim1*-ASHCE to investigate its regulatory role in *Sim1* expression and flight feather development. By disrupting this conserved non-coding element, the study aimed to determine whether perturbation of *Sim1* regulation affects flight feather morphogenesis. The resulting genome-edited (GE) chickens serve as a valuable model for exploring the role of non-coding regions in shaping complex phenotypes, offering key insights into the evolutionary and functional significance of enhancers in avian diversity.

MATERIALS AND METHODS

Ethical statement

All animal care and experimental procedures were conducted in accordance with regulations for animal experimentation and were approved by the Animal Care and Use Committees of Yunnan Agricultural University (Approval Code: YAUACUC01) and Osaka Metropolitan University (S0086).

Single-guide RNA (sgRNA) and CRISPR/Cas9 plasmid construction targeting *Sim1*-ASHCE

The 284 bp potential enhancer sequence of ASHCE is located within the eighth intron of the *Sim1* gene on chromosome 3 (positions 70396108–70396391 in the ICGSC Gallus_gallus-4.0/galGal4 reference or 70986326–70986609 in GRCg6a/galGal6). To disrupt this sequence, three sgRNA targets (sgRNA-#1, -#2, -#3) were designed within the 284 bp region and its flanking sequences using CRISPRdirect (http://crispr.dbcls.jp/) (Naito et al., 2015) (Supplementary Table S1). Each sgRNA oligonucleotide was synthesized with the addition of CACCG to the 5' flanking sequence of the sense oligonucleotide, AAAC to the 5' flanking sequence of the antisense oligonucleotide, and C to the 3' flanking sequence to facilitate ligation into the *Bbs*I site of the pSpCas9(BB)-2A-Puro plasmid (pX459; plasmid #48139, Addgene, USA). The annealed oligonucleotides were independently inserted into the pX459 vector. The resulting plasmids, designated pX459-*Sim*EN-sgRNA#1, -#2, and -#3, were confirmed by sequencing using the U6 promoter primer (U6-F, 5'-ACTATCATATGCTTACCGTAAC-3').

Preparation of PGCs

A primary cultured male PGC line (#P28) derived from Piao chicken and cryopreserved in liquid nitrogen in our previous study (Kinoshita et al., 2024) was utilized as the donor cell source. This line was established from a single embryonic blood sample collected at the HH15 stage (Hamburger & Hamilton, 1992) and cultured as described previously (Kinoshita et al., 2024). In brief, the basal culture medium was prepared by supplementing avian knockout Dulbecco's Modified Eagle Medium (DMEM) with 1×GlutaMAX (Life Technologies, USA), 1×nonessential amino acids (Life Technologies, USA), 1×EmbryoMax nucleosides (Merck Millipore, Germany), 1.2 mmol sodium pyruvate (Life Technologies, USA), and 0.1 mmol β-mercaptoethanol (Life Technologies, USA). FAOTcs medium was prepared by supplementing basal medium with 0.2% chicken serum, 10 μg/mL conalbumin (Sigma-Aldrich, USA), 0.2% ovalbumin,

0.01% sodium heparin (Sigma-Aldrich, USA), 4 ng/mL FGF2 (PeproTech, USA), and 25 ng/mL activin A (PeproTech, USA). PGCs were cultured at 37.8°C in a humidified atmosphere containing 5% CO_2 and 11%–13% O_2, reflecting the high-altitude environmental conditions.

Generation of *Sim1*-ASHCE GE PGC lines using CRISPR/Cas9

Three combinations of pX459 plasmid vectors (pX459-*Sim1*EN-sgRNA#1/-#2, -#2/-#3, -#1/-#3) were transfected into 1×10^6 PGCs using Lipofectamine 3000 (Thermo Fisher Scientific, USA). Transfection was performed in Opti-MEM I medium. Following centrifugation at 1 500 r/min for 5 min at room temperature, the cells were resuspended in FAOTcs medium and incubated for 24 h at 37.8°C and 5% CO_2. Post-transfection, selection was performed using puromycin (1 μg/mL) for 72 h, after which surviving PGCs were cultured in FAOTcs medium for an additional 3–6 weeks.

Mutation confirmation and analysis

Genomic DNA was extracted from the GE PGC lines using QuickExtract DNA Extraction Solution (Lucigen, USA). An 830 bp genomic region encompassing the *Sim1*-ASHCE sequence was amplified by polymerase chain reaction (PCR) using KOD FX DNA polymerase (TOYOBO, Japan) and primers ASHCE_TF1 and ASHCE_TR1 (Supplementary Table S2). The PCR products were analyzed by agarose gel electrophoresis. Bands indicating potential deletions were excised and the exact mutation site was determined by Sanger sequencing. Additionally, small mutations were detected using the T7 endonuclease I (T7EI) assay, with 100 ng of PCR product mixed with 10 units of T7 endonuclease I (Vazyme, China) and analyzed by 1.5% agarose gel electrophoresis. Targeting efficiency was assessed by measuring band intensities with Image Lab v.5.0 (BioRad Laboratories, USA).

Transplantation of GE PGCs and culture of recipient embryos

The GE PGC line (#P28-*Sim1*EN-#1/#2GE-A) was selected to generate germline chimeras. Approximately 1 μL (4 000–4 500 cells) of these PGCs was microinjected into the dorsal aorta of HH14–16 stage recipient embryos derived from a crossbred population (CP: Chahua×Phoenix bantam). CP embryos were selected for their heterosis effect, which improves hatchability during surrogate eggshell culture. Embryos were transferred into surrogate eggshells (Perry, 1988) and incubated at 37.8°C until hatching.

Screening of donor PGC-derived chicks

Recipient chicks were raised to sexual maturity and screened for the presence of the Piao-derived fibromelanosis (*Fm*)-specific PCR amplicon in sperm, as reported in our previous study (Kinoshita et al., 2024). Positive males were mated with 3–10 wild-type (WT) hens from a crossbred population (Chahua×Serama, CS). CS hens were selected based on small size, reasonable egg-laying performance, and normal wing and tail feather phenotypes. G1 progeny were screened for autosomal dominant mutations, including rumplessness (*Rp*) and *Fm*, present in the donor PGC line (#P28) but not in recipient CP males and WT CS hens. Detection of target region mutations in donor PGC-derived chicks was verified by PCR amplicon size analysis and Sanger sequencing. PCR amplification was performed in a 10 μL total volume containing 1.0 μL of blood lysis sample, 0.01 μmol/L each primer (ASHCE_TF1 and ASHCE_TR2 listed in Supplementary Table S2), and 5 μL of ESTaq Master Mix (Tiangen Biotech, China), according to the manufacturer's instructions.

Feather development analysis

Feather development was evaluated in *Sim1*-ASHCE GE and WT chickens across multiple developmental stages, with a primary focus on the G2 generation. Flight feather development was assessed at embryonic day 11 (E11) using G2 GE and WT samples (n=2 each). The total number of primary and secondary flight feathers was counted, and forelimb size, morphology, and feather structure were observed under a stereomicroscope. Post-hatching observations were conducted on G2 chicks from days 1 to 7. The number of primary and secondary flight feathers was recorded for homozygous GE (n=30), heterozygous GE (n=15), and WT (n=20) chicks. Flight feather elongation was visually assessed, and feather development was further monitored in G2 GE and WT chicks from 3 to 10 weeks post-hatching, including observations of flight, covert, and tail feathers. In adult G2 chickens, the normal complement of flight feathers (10 primaries and 14 secondaries) and fertility were evaluated to confirm the absence of phenotypic abnormalities. Observations of G3 and G4 generations were conducted to confirm the continuity of normal feather development and fertility.

Detection of sex-linked dominant late feathering (*K*) mutation by multiplex PCR

The wild-type (k^+) allele on chromosome Z contains the *PRLR* and *SPEF2* genes, whereas the late feathering (LF; *K*) allele carries partial duplications of these genes (*dPRLR* and *dSPEF2*) in addition to the original genes (Supplementary Figure S1). A multiplex PCR assay was designed based on the breakpoint junction within the duplicated regions, as previously described by Elferink et al. (2008). This assay utilized three primers: two forward primers (FD1 and FD2) and a common reverse primer (RV) (Supplementary Table S1). Amplification of the *K* allele generated two products: a 403-bp fragment spanning the breakpoint junction and a 342-bp fragment common to both alleles. In contrast, the wild-type allele produced only the 342-bp product. This assay was employed to detect the LF mutation in donor Piao PGCs, CS females derived from mating experiments, and G1 progeny. Genomic DNA was extracted from PGCs or blood samples using standard protocols. An Ingie chicken exhibiting the LF phenotype was included as a positive control. Multiplex PCR reactions were conducted in a total volume of 10 μL, containing 1 μL of genomic DNA (~50 ng/μL), 0.01 μmol/L each primer, and 5 μL of ES-Taq Master Mix (Tiangen Biotech, China). PCR products were analyzed by agarose gel electrophoresis.

RNA isolation and reverse transcription-quantitative real-time PCR (RT-qPCR) analysis

Forelimb samples were collected from E8 WT and GE embryos and stored in RNAlater (Ambion, USA). Total RNA was extracted using TRIzol reagent (Invitrogen, USA), and RNA quality and concentration were measured with a NanoDrop spectrophotometer (Thermo Fisher Scientific, USA). cDNA was synthesized from 1 μg of total RNA using a PrimeScript RT-PCR Kit (Takara, Japan) and oligo dT primers. RT-qPCR was performed using TB Green Premix Ex Taq II (Takara Bio, Japan) and the CFX96 Real-Time PCR Detection

System (Bio-Rad Laboratories, USA). *Sim1* gene expression was normalized to that of *GAPDH*. The primers used are listed in Supplementary Table S2. RT-qPCR was conducted in triplicate, with the mean mRNA expression values used for data analysis. Gene expression levels were analyzed using the 2-ΔΔCT method (Schmittgen & Livak, 2008). Statistical analysis between two groups was performed using Welch's *t*-test in Microsoft Excel (Microsoft, USA), with data presented as mean±standard deviation (SD) and the significance threshold set at *: P<0.05.

In situ hybridization of tissue sections

The *Sim1* cDNA plasmid was kindly provided by Dr. Tamura (Seki et al., 2017). *In situ* hybridization was performed on paraffin-embedded tissue sections from E8 WT chick forelimbs. Paraffin sections (10 μm) were deparaffinized by washing in xylene for 5 min three times, followed by rehydration through graded ethanol/phosphate-buffered saline (PBS) series (100%, 90%, and 70%, each for 5 min) and a 10 min wash in PBT (0.5% Tween-20/PBS). Sections were then treated with 1 μg/mL Proteinase K/PBT for 7 min, washed three times for 1 min with PBT, and refixed in 4% PFA/PBT for 20 min. After two additional 1-min PBT washes, hybridization was performed using denatured *Sim1* DIG-labeled RNA probes (1 μg/mL) in hybridization buffer (750 μL of formamide, 370 μL of 20×SSC (pH 5.0), 3.75 μL of tRNA (20 μg/mL), 1.5 μL of heparin (50 μg/mL), 75 μL of 10% SDS, and 300 μL of Depc H_2O) and denatured at 95°C for 2 min. Each slide was covered with 100 μL of probe solution, sealed with parafilm, and incubated overnight at 65°C. The next day, the slides were washed twice for 30 min with wash solution (250 mL of formamide, 50 mL of 20×SSC (pH 5.0), and 200 mL of H_2O) pre-warmed to 65°C, followed by a 10 min wash with 50% wash solution and cooling to room temperature. The samples were blocked with blocking solution for 1 h, washed twice with PBT, incubated overnight at 4°C with 100 μL of 1/1 000 diluted Anti-Digoxigenin-AP Fab fragments in blocking solution (10% blocking reagent/MAB 30 mL, sheep serum 30 mL, TBST 90 mL), and sealed with parafilm. The next day, the slides were washed three times (5 min each) with 2 mmol/L Levamisole/TBST, then equilibrated in NTMT buffer (6 mL of 5 mol/L NaCl, 15 mL of 1 mol/L $MgCl_2$, 30 mL of 1 mol/L Tris-HCl (pH 9.5), 1.5 mL of 20% Tween 20, 300 μL of 2 mol/L levamisole, and 250 μL of H_2O) for 5 min. The samples were then incubated in color development solution (52.5 μL of 100 mg/mL NBT and 53 μL of 50 mg/mL BCIP in 150 mL of NTMT) in the dark until the desired color developed. Once staining was confirmed, the slides were washed with PBT for 30 min and fixed in 4% paraformaldehyde (PFA)/PBT for 30 min. Finally, the samples were washed with PBT and mounted with PVA mounting medium (6 g of glycerol, 6 mL of 0.2 mol/L Tris-HCl (pH 8.5), and 1.2 mg of polyvinyl alcohol in H_2O) before covering with a coverslip.

Off-target candidate selection and analysis

Three highly specific sgRNA sequences (sgRNA#1–#3) targeting the *Sim1*-ASHCE region were selected using CRISPRdirect (http://crispr.dbcls.jp/) based on the chicken genome database (ICGSC Gallus_gallus-4.0/galGal4) (Supplementary Table S1). Off-target candidates (OTCs) were identified from CRISPRdirect search results (Supplementary Table S1). No OTCs were detected for sgRNA#1 at the 20-mer+PAM or 12-mer+PAM levels, reflecting high sequence specificity. However, six OTCs located on different chromosomes were randomly selected from the 1 510 OTCs (excluding the on-target sequence) identified for the 8-mer+PAM region of sgRNA#1 (Supplementary Table S2). For sgRNA#2, 11 OTCs (excluding the on-target sequence) were identified in the 12-mer+PAM region, and five OTCs located on different chromosomes were randomly selected for further analysis (Supplementary Table S2). Genomic DNA extracted from GE PGCs (#P28-*Sim1*EN-#1/#2GE-A) and original PGCs (#P28) was PCR-amplified using the primers listed in Supplementary Table S1. Sanger sequencing was performed for each PCR product using the same primers, and sequence data were analyzed using ATGC sequence assembly software v.3.0 (Genetyx, Japan). Furthermore, the sequences were compared to the reference genome (ICGSC Gallus_gallus-4.0/galGal4) using the Chicken BLAT search tool (https://genome.ucsc.edu/cgi-bin/hgBlat) (Kent, 2002).

RESULTS

Establishment of *Sim1*-ASHCE-disrupted PGC lines

To disrupt the 284 bp *Sim1*-ASHCE region, three highly specific target sequences were selected within and flanking the *Sim1*-ASHCE (Figure 1A; Supplementary Table S1). Two sgRNAs were combined to induce deletions, transfecting three pairs of pX459 plasmids (pX459-*Sim1*EN-sgRNA#1/-#2, -#2/-#3, -#1/-#3) into male Piao PGC lines (#P28), followed by puromycin selection. The transfected cells were then expanded for 3–6 weeks. Despite multiple transfection attempts, PGC numbers often declined within weeks post-transfection and drug selection, resulting in frequent failure to establish GE PGC lines. Nevertheless, four GE PGC lines were successfully generated: two from the #1/#2 combination (#1/#2-A and #1/#2-B), one from the #2/#3 combination, and one from the #1/#3 combination. Mutations were initially assessed by PCR amplicon size analysis and T7EI assay (Figure 1B, C). Three lines (#1/#2-A, #1/#2-B, and #2/#3) exhibited clear biallelic deletions in the target region, producing PCR amplicons of 500–600 bp, approximately 200–300 bp shorter than the 830 bp WT band (Figure 1B). In contrast, the #1/#3 line produced amplicons similar in size to the WT, suggesting the absence of discernible deletions. T7EI assays confirmed high cleavage efficiencies in the #1/#2-A, #1/#2-B, and #2/#3 lines (99.9%, 99.7%, and 99.7%, respectively), with only faint residual WT bands. Conversely, cleavage efficiency in the #1/#3 line was only 62.2% (Figure 1C). Sequencing the PCR products confirmed deletions of approximately 260 bp and 310 bp in the #1/#2-A, #1/#2-B, and #2/#3 PGC lines (Figure 1D). The #1/#3 line, however, failed to yield a GE PGC line completely lacking the *Sim1*-ASHCE region, despite repeated transfection attempts. Ultimately, the GE PGC line (#P28-*Sim1*EN-#1/#2GE-A), established using the sgRNA#1/#2 set and with sufficient cell numbers, was selected to generate *Sim1*-ASHCE GE chickens.

Progeny testing of recipient males to produce donor GE PGC-derived chicks

Donor GE PGCs (#P28-*Sim1*EN-#1/#2GE-A) were transplanted into 58 HH14–16-stage embryos from crossbred chickens (CP: Chahua×Phoenix bantam), resulting in the successful hatching of 14 recipient chicks. Among these, four males and six females reached sexual maturity, with the remaining four chicks dying soon after hatching. The four surviving male recipients (#30, #32, #43, and #44) were used

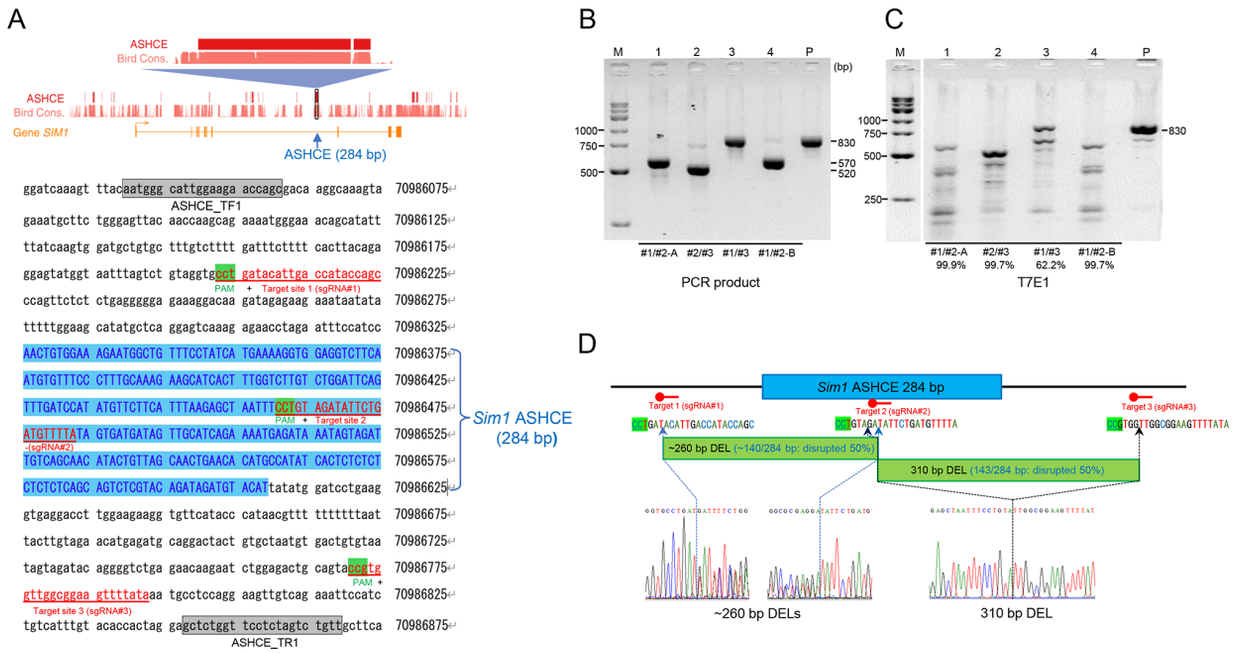

Figure 1 Establishment of *Sim1*-ASHCE disrupted (GE) PGC lines via the CRISPR/Cas9 system

A: Schematic representation of gene structure of *Sim1*, as well as base-wise conservation scores for ASHCEs from Seki et al. (2017). Area containing the highest-scoring 284 bp *Sim1*-ASHCE is enlarged. The 284 bp potential enhancer sequence of *Sim1*-ASHCE (blue) is located at positions 70 986 326–70 986 609 (GRCg6a/galGal6), within the eighth intron of *Sim1* on chromosome 3. Three sgRNA sequences and protospacer adjacent motif (PAM) sequences are underlined in red and light green, respectively. Two primers underlined in black were employed to amplify the target region (830 bp), which included the 284 bp ASHCE and three target sequences. B, C: PCR products for the intron 8 target region of *Sim1* were amplified using each bulk DNA sample from *Sim1*-ASHCE GE PGC lines with three sets of sgRNAs (#1/#2, #2/#3, and #1/#3) (B), and cleavage efficiency was assessed by the T7EI assay (C). P: Genomic DNA sample, derived from the original donor Piao PGC♂#28. D: Sanger sequencing analysis of 570 bp and 520 bp PCR products with biallelic deletions at the target region for two GE PGC lines (#1/#2-A and #2/#3). Sequence chromatograms show a 260 bp deletion in target regions for #1/#2-A GE PGC (left) and a 310 bp deletion in target region for #2/#3 GE PGC (right). Both GE PGC lines exhibited disruption of approximately 50% of the 284 bp *Sim1*-ASHCE sequence (140/284 bp for #1/#2-A GE PGC and 143/284 bp for #2/#3 GE PGC). Sequences of the three sgRNAs and PAM sites, underlined in light green, are presented. Blue and black dashed arrows indicate CRISPR/Cas9-induced mutation sites.

for progeny testing with WT hens (CS), producing a total of 433 G1 chicks (Figure 2A; Table 1). The G1 chicks were classified as donor GE PGC-derived or recipient-derived based on two autosomal dominant traits, *Rp* and *Fm*, both carried by the donor Piao PGC line (#P28, *Rp*/*Rp* *Fm*/*fm*$^+$), following previously established methods (Kinoshita et al., 2024). Of the four males, only two (#32 and #43) successfully produced donor-PGC derived chicks. Male #32 produced 58 chicks, 13 (22.4%) of which exhibited tailbone defects (*Rp*/*rp*$^+$) and occasional black skin (*Fm*/*fm*$^+$), indicating derivation from donor GE PGCs. Male #43 produced 282 chicks, with seven (2.5%) showing the same phenotypes. In contrast, 93 chicks from males #30 and #44 (34 and 59 chicks, respectively) exhibited normal phenotypes (*rp*$^+$/*rp*$^+$ and *fm*$^+$/*fm*$^+$), indicating recipient origin (Figure 2A). Further genotyping of 20 G1 chicks confirmed the presence of both the GE (~260 bp) and WT alleles (523 bp) in all donor-derived chicks (Figure 2B). These 20 G1 progeny consisted of nine males and 11 females. Sanger sequencing revealed three distinct deletions (257 bp, *n*=3; 258 bp, *n*=12; and 260 bp, *n*=5) within the target region, accounting for approximately 50% (140–143 bp) of the 284 bp *Sim1*-ASHCE sequence (Figure 2C).

Production of homozygous G2 chicks from heterozygous G1 mating

A total of 194 G2 chicks, including embryos that died before hatching, were produced by mating heterozygous G1 birds from Groups 1 and 2. Group 1, consisting of seven G1 females and two G1 males, produced 81 G2 chicks, while Group 2, consisting of two G1 females and two G1 males, produced 113 G2 chicks (Table 2). The *Sim1*-ASHCE genotypes of the G2 chicks were determined by PCR analysis (Figure 3A). Group 1 progeny segregated into 15 WT, 42 heterozygous, and 24 homozygous chicks, which did not significantly differ from the expected 1:2:1 Mendelian ratio (χ^2=2.11, *P*=0.36). Similarly, Group 2 progeny segregated into 26 WT, 56 heterozygous, and 31 homozygous chicks, with no significant difference from the expected 1:2:1 ratio (χ^2=0.45, *P*=0.80) (Table 2).

Analysis of *Sim1* expression in *Sim1*-ASHCE GE embryos

To assess the impact of the partial deletion (50%) of the 284 bp *Sim1*-ASHCE sequence, *Sim1* gene expression was compared between homozygous GE and WT embryos using forelimb samples from G2 embryos at the HH34 (E8) stage. RT-qPCR analysis revealed a significant reduction in *Sim1* expression in GE embryos (*n*=7) compared to WT embryos (*n*=7) at day 8, exhibiting levels 0.32-fold that of WT expression (mean±SD: 0.40±0.11 in GE vs. 1.25±0.69 in WT, *P*=0.018) (Figure 3C). *In situ* hybridization of zeugopod tissue sections was performed to confirm the localization of *Sim1* expression in E8 WT embryos. *Sim1* signals were detected in the ventral mesenchyme surrounding the flight feather bud but were absent within the bud itself (Figure 3D). Weak

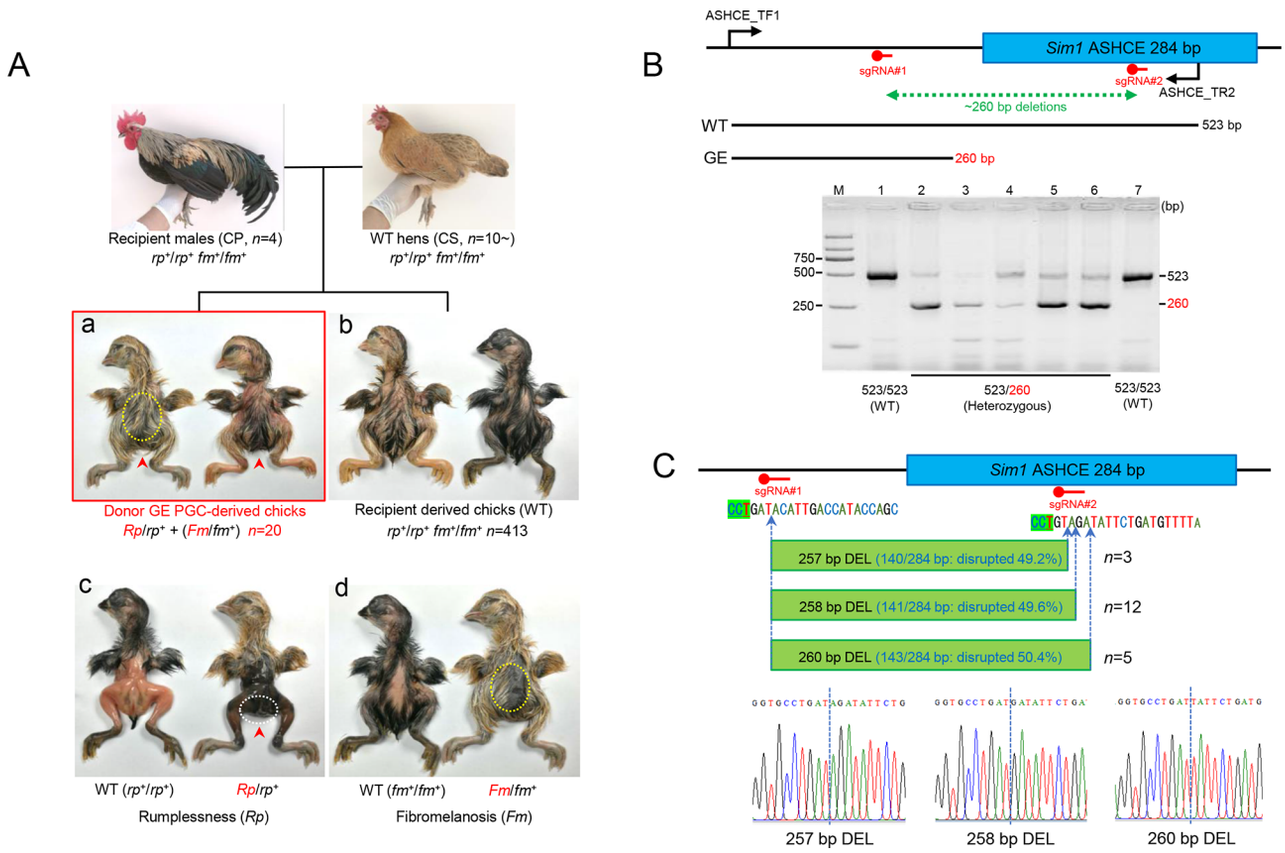

Figure 2 Progeny testing of recipient (putative germline chimeric) males and WT hens

A: Classification of G1 chicks from mating of male recipients (CP) and WT hens (CS). Donor Piao GE PGC-derived chicks exhibit a tailbone defect (rumplessness, *Rp*/*rp*$^{+}$) as indicated by red arrowheads and occasionally a black skin (Fibromelanosis, *Fm*/*fm*$^{+}$) phenotype, as indicated by yellow dashed circles (a). In contrast, WT chicks (*rp*$^{+}$/*rp*$^{+}$ *fm*$^{+}$/*fm*$^{+}$) derived from recipient male and CS hens do not carry either mutation (b). Donor GE PGC-derived chicks with *Rp* mutation can be distinguished from WT chicks by both phenotypic observation and palpation due to their lack of a tailbone, as indicated by white dashed circle and red arrowhead (c). Similarly, some chicks from donor GE PGCs can be distinguished from WT chicks by a black skin phenotype, as donor Piao PGCs are heterozygous for *Fm* mutation (d). B: PCR-based genotyping of 260 bp deletion in the target region in G1 chicks. Intron 8 target region, which included a portion of 284 bp *Sim1*-ASHCE, was amplified using primers ASHCE-TF1 and ASHCE-TR2. WT chicks exhibited a single 523 bp product, whereas all donor GE PGC-derived G1 chicks with tailbone defects demonstrated 523/~260 bp heterozygous bands, derived from both WT and GE alleles. C: Sequence analysis of *Sim1*-ASHCE target region for GE alleles of G1 chicks. Analysis of 260 bp deletion band for GE alleles from GE PGC-derived G1 chicks revealed the presence of three distinct deletion mutations of varying sizes: 257 bp (*n*=3), 258 bp (*n*=12), and 260 bp (*n*=4). CRISPR/Cas9-induced deletion mutations occurred at the same site on sgRNA#1 and at three different sites on sgRNA#2, as indicated by blue dashed arrows in WT sequences. PAM sequences are indicated in green. Sequence chromatograms demonstrate the presence of three types of GE alleles, each exhibiting a 257, 258, or 260 bp deletion, as indicated by blue dashed lines.

Table 1 Frequencies donor genome-edited PGC-derived chicks produced from recipient males mated with WT hens (Progeny Test)

Recipient males	Donor GE PGC line	Number of mated hens (WT)	Set of eggs	Hatched chicks	Number of donor GE PGC-derived progeny (%)
#30♂	♂#P28-*Sim1*EN-#1/#2GE-A	5	50~	34	0 (0%)
#32♂		8	80~	58	13 (22.4%)
#43♂		10	380~	282	7 (2.5%)
#44♂		5	70~	59	0 (0%)
Total		-	580~	433	20 (4.6%)

GE: Genome-edited; PGC: Primordial germ cell; WT: Wild-type.

expression was also observed in the ulna and radius, while no expression was detected in nerve or muscle tissues at this developmental stage.

Analysis of flight feather phenotypes in *Sim1*-ASHCE GE chickens

Flight feather development was examined in G2 *Sim1*-ASHCE GE (*n*=2) and WT embryos (*n*=2) at embryonic day 11 (E11). Both groups exhibited identical numbers of flight feathers (10 primaries and 14 secondaries), with no observable differences in forelimb size, morphology, or feather structure (Figure 3A). Post-hatching observations from days 1–7 revealed consistent flight feather numbers among homozygous (*n*=30), heterozygous (*n*=15), and WT chicks (*n*=20) (Figure 4C; Figure 3B). However, considerable individual variation was

Table 2 Segregation of *Sim1*-ASHCE genotypes in G2, G3, and G4 progenies

Matings (genotypes/generation/sex/numbers)	No. of progeny	Genotypes of *Sim1*-ASHCE target region			Expected ratio	χ^2	*P*
		WT (523 bp/523 bp, WT/WT)	Heterozygous (523 bp/260 bp, WT/DEL)	GE (260 bp/260 bp, DEL/DEL)			
G2 progeny (G1×G1)							
Group1: Het. G1♀ (*n*=7)×Het. G1♂ (*n*=2)	81	15	42	24	1:2:1	2.11	0.9<*P*<0.1
Group2: Het. G1♀ (*n*=2)×Het. G1♂ (*n*=2)	113	26	56	31	1:2:1	0.45	0.9<*P*<0.1
Total	194	41	98	55	1:2:1	2.04	0.9<*P*<0.1
G3 progeny (G2×G2)							
GE G2♀ (*n*=2)×GE G2♂ (*n*=1)	16	–	–	16	–	–	–
G4 progeny (G3×G3)							
GE G3♀ (*n*=1)×GE G3♂ (*n*=1)	7	–	–	7	–	–	–

Bp: Base pair; DEL: Deletion; G1: 1st generation; G2: 2nd generation; G3: 3rd generation; G4: 4th generation; GE: Genome-edited; Het.: Heterogenous; *P:* Level of significance; WT: Wild-type. –: Not available.

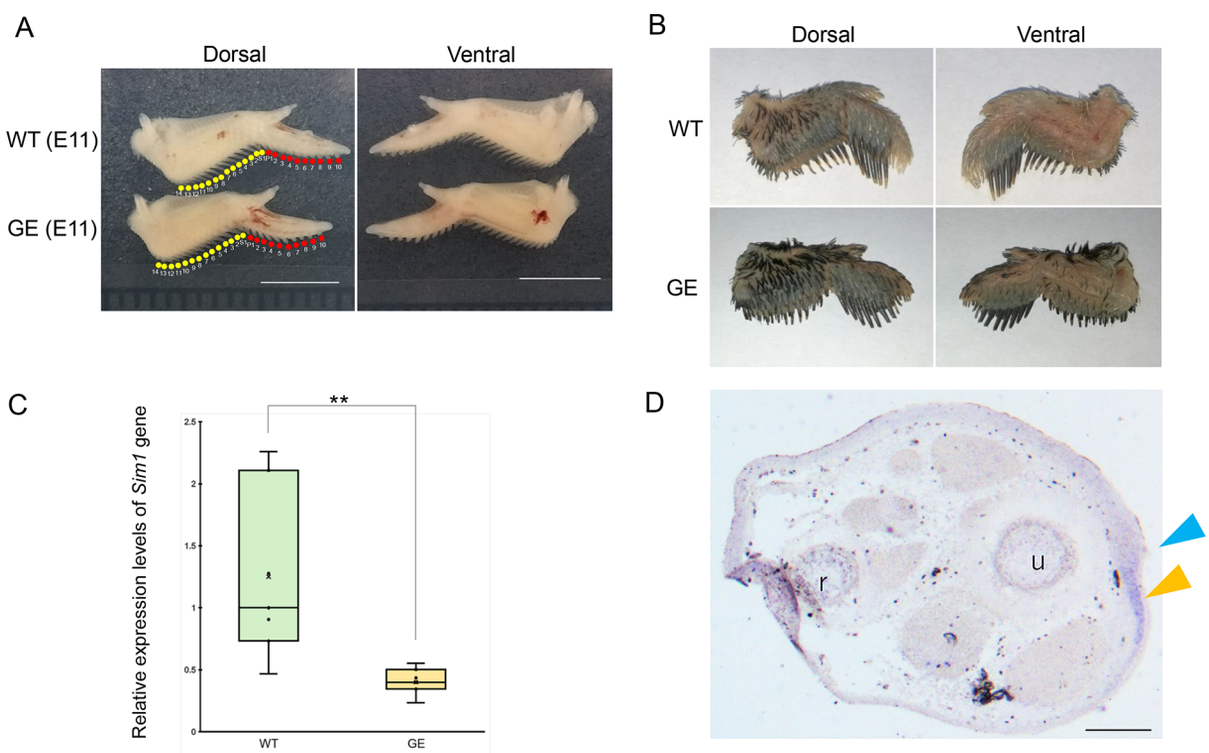

Figure 3 Forelimb morphology and *Sim1* gene expression in *Sim1*-ASHCE GE embryos

A: Morphology of forelimbs of day 11 (E11) embryos, showing no observable differences between GE and WT embryos in overall size, shape, or flight feathers of forelimbs. Upper image shows E11 WT embryo wing, and lower image shows E11 GE embryo wing. Red circles and white numbers (P1–10) indicate primary flight feathers, while yellow circles and white numbers (S1–14) indicate secondary flight feathers. Scale bars: 5 mm B: No notable discrepancies were identified in the number or distribution of flight feathers or down feathers between WT and GE G2 embryos at the 20–21 day stage prior to hatching. Tips of down and flight feathers were trimmed for easier observation. However, individual variations in the degree of flight feather development were observed within the G2 progeny, which were not associated with the *Sim1*-ASHCE genotype (see Supplementary Figure S1). C: *Sim1* gene expression in the forelimbs of day 8 (E8) embryos. Relative expression levels of *Sim1* were compared between WT (*n*=7) and GE (*n*=7) embryos. Data were analyzed using Welch's *t*-test. There was a significant difference between the WT and GE embryos (*P*=0.018). Horizontal lines represent median, while cross represents mean expression value. Mean expression levels in WT and GE groups were 1.25±0.69 and 0.40±0.11, respectively. Data are represented as mean±SD. **: *P*<0.01. D: *Sim1* expression in cross section at zeugopod area in E8 WT chick embryo. Top shows dorsal side, and bottom shows ventral side. Orange arrowhead shows *Sim1* expression. Light blue shows budding structure of flight feather bud. u: Ulna, r: Radius. Scale bars: 200 μm.

noted in secondary flight feather elongation. Some individuals exhibited a delay in secondary flight feather development by day 5 post-hatching (Supplementary Figure S1), although this delay was not associated with the *Sim1*-ASHCE genotype. Similar delays have previously been observed in Piao chicks derived from donor Piao PGCs (Kinoshita et al., 2024), suggesting the involvement of spontaneous mutation in the donor Piao PGCs. To investigate the genetic cause, the presence of the sex-linked dominant late feathering (*K*) mutation on the Z chromosome was examined. However, the *K*-specific 403 bp amplicon was absent in donor Piao PGCs, CS females, and G1 individuals, with only the common 342 bp fragment of *K* and k^+ alleles detected (Supplementary Figure S1). These results indicate that the delayed feathering

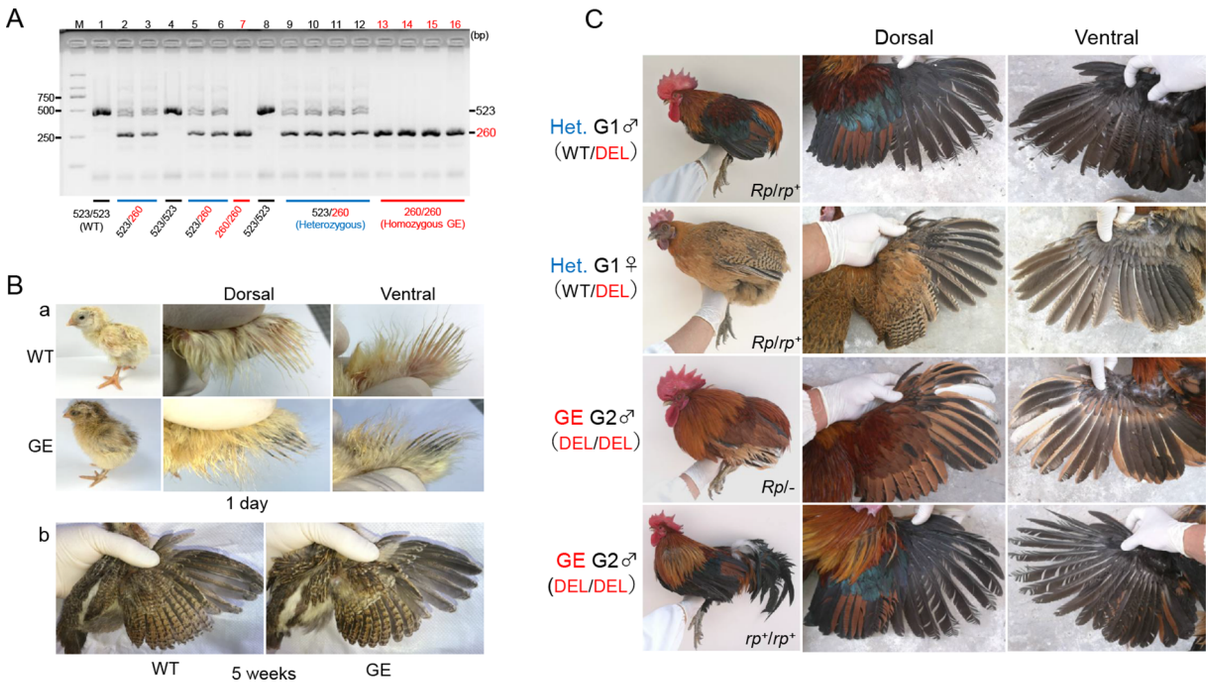

Figure 4 Generation of *Sim1*-ASHCE GE chickens and their phenotypic characteristics

A: Genotyping of 260 bp deletion within the target region of GE PGCs in G2 chicks using primers ASHCE-TF1 and ASHCE-TR2, as described in Figure 2B. G2 chicks were segregated into three genotypes. WT genotype (WT/WT) exhibited a 523 bp band (lanes 1, 4, and 8), heterozygous genotype (WT/DEL) showed two bands, 523 bp and 260 bp (lanes 2, 3, 5, 6, and 9–12), and homozygous GE genotype (DEL/DEL) exhibited a 260 bp band (lanes 7 and 13–16). B: Flight feather phenotypes of WT and GE chicks at 1 day and 5 weeks after hatching. Flight feather phenotypes of WT and GE G2 chicks at 1 day post-hatching (a) and flight feather phenotypes of WT and GE G2 chicks (different individuals) at 5 weeks of age (b) are presented. C: Flight feather phenotypes of heterozygous (WT/DEL) and homozygous (DEL/DEL) GE chickens at adult stage. Mature heterozygous G1 chickens exhibited normal development of flight feathers in both adult males and females. Similarly, homozygous GE G2 chickens exhibited normal feather development. Mature homozygous GE chickens, which lacked the *Rp* mutation, also exhibited normal development of tail feathers.

phenotype was not attributable to the *K* mutation. The retarded-tardy feathering (*t*) mutation, which phenotypically resembles *K*, remains a potential cause, although its responsible gene has not yet been identified, precluding further investigation. During the 3–10 weeks post-hatching period, no phenotypic differences were observed between homozygous GE and WT chicks in flight feathers or other feather types, including covert and tail feathers (Figure 4B). Adult GE chickens exhibited the normal complement of 10 primary and 14 secondary flight feathers, regardless of *Sim1*-ASHCE genotype or the presence of delayed feather mutations (Figure 4C). Additionally, G3 and G4 progeny from homozygous GE chickens displayed normal fertility and feather development, consistent with observations in earlier generations (Table 2). These findings indicate that *Sim1*-ASHCE deletion does not affect flight or tail feather formation in chickens.

Evaluation of off-target effects in CRISPR/Cas9-edited *Sim1*-ASHCE GE PGCs

Potential OTCs within the 20-mer, 12-mer, and 8-mer+PAM (NGG) motifs were assessed for three target sequences (sgRNA#1, sgRNA#2, and sgRNA#3) using CRISPRdirect (http://crispr.dbcls.jp/) based on the chicken genome (ICGSC Gallus_gallus-4.0/galGal4) (Supplementary Table S2). No OTCs were detected within the 20-mer+PAM regions for any of the three sgRNAs, indicating high targeting specificity. To further evaluate potential off-target effects, six OTCs were randomly selected from 1 510 candidates in the sgRNA#1 8-mer+PAM region, and five OTCs were selected from 11 candidates in the sgRNA#2 12-mer+PAM region (Supplementary Table S2). These candidate regions were amplified using genomic DNA from the GE PGCs (#P28-*Sim1*EN-#1/#2GE-A) and original PGCs (#P28) (as controls). PCR amplification and sequencing revealed no mutations in any of the selected OTCs or within approximately 50 bp of their flanking regions. Comparative analysis against the reference genome (ICGSC Gallus_gallus-4.0/galGal4) further confirmed the absence of CRISPR/Cas9-induced mutations (Supplementary Figure S2). Several single nucleotide polymorphisms (SNPs) and repeat polymorphisms were identified within the PCR-amplified regions but were located outside the OTC sequences and their immediate flanking regions, indicating spontaneous genetic variations in the Piao line unrelated to genome editing (Supplementary Figure S3).

DISCUSSION

This study investigated the functional significance of a 284 bp avian-specific sequence (*Sim1*-ASHCE) located within the eighth intron of *Sim1*, previously hypothesized to contribute to the evolutionary development of flight feathers (Seki et al., 2017). Using CRISPR/Cas9-mediated genome editing, *Sim1*-ASHCE-deficient GE PGC lines and GE chickens were generated. Although complete deletion of the ASHCE was not achieved —likely due to limitations in sgRNA cleavage efficiency, sgRNA pairing, PGC condition, and post-transfection culture stability—the successful establishment of GE chickens harboring partial (50%) deletions enabled

preliminary functional assessment. Future optimization of genome editing protocols will be essential to establish PGC lines completely lacking *Sim1*-ASHCE and to fully assess its functional role.

Sim1-ASHCE has been characterized as a tissue-specific enhancer with evolutionary significance in birds (Seki et al., 2017). Reporter assays in mouse embryos have demonstrated that the 284 bp *Sim1*-ASHCE sequence exhibits enhancer activity, implicating its involvement in flight feather development. Consistent with these findings, RT-qPCR analysis in this study revealed that GE chickens carrying partial *Sim1*-ASHCE deletions exhibited markedly reduced *Sim1* expression (0.32-fold compared to WT) in E8 embryos (HH34 stage). This reduction confirms that *Sim1*-ASHCE functions as an active enhancer during forelimb development. Despite the substantial decrease in *Sim1* expression, no morphological abnormalities were detected in the flight or tail feathers of *Sim1*-ASHCE GE chickens. Notably, GE and WT chickens exhibited identical numbers of primary (n=10) and secondary (n=14) flight feathers, with full development of covert feathers and normal feather structure across all generations examined. These findings suggest that partial disruption of *Sim1*-ASHCE does not impair flight feather morphogenesis, likely due to genetic redundancy. Enhancer redundancy has been increasingly recognized as a mechanism conferring phenotypic resilience to regulatory perturbations in mammals, with similar compensatory mechanisms potentially existing in avian feather development (Osterwalder et al., 2018). Wu et al. (2018) demonstrated that multiple regulatory modules are critical for scale-to-feather conversion, emphasizing the complexity of feather morphogenesis. Feather development may thus depend on a network of regulatory elements that can mitigate the effects of individual enhancer deletions, including *Sim1*-ASHCE. The normal development of flight feathers in *Sim1*-ASHCE GE chickens, despite reduced *Sim1* expression, may also be attributed to genetic compensation mechanisms. As proposed by El-Brolosy & Stainier (2017), such mechanisms may involve the up-regulation of functionally redundant genes or the activation of alternative signaling pathways. In this context, compensatory responses could occur through the recruitment of other enhancers or transcription factors or through parallel pathways mediated by *Zic* family members (*Zic1*, *Zic3*, *Zic4*), known modulators of *Shh* signaling (Busby et al., 2020). Moreover, conserved enhancer landscapes surrounding *Sim1* have been identified in mammals (Kim et al., 2014), raising the possibility that additional enhancers in the avian genome maintain *Sim1* expression following partial ASHCE deletion.

Interestingly, *in situ* hybridization analysis of E8 WT embryos revealed that *Sim1* expression was localized predominantly within the posterior mesenchyme adjacent to the developing flight feather buds, rather than within the feather buds themselves. This pattern is consistent with previous observations reporting *Sim1* expression along bones and nerves in E10 embryos (Busby et al., 2020). Although slight *Sim1* expression was detected in the ulna and radius, its functional significance remains unclear. Notably, while *Sim1* is known to be transiently expressed in limb muscle progenitor cells during early embryogenesis, it was no longer detectable in either muscle or nerve tissues by the HH34 (E8) stage. These findings suggest that *Sim1* activity may be confined to surrounding mesenchymal tissues, rather than directly influencing feather formation. The absence of any flight feather abnormalities in *Sim1*-ASHCE GE chickens further supports the notion that *Sim1*, specifically the deleted *Sim1*-ASHCE enhancer, is not essential for feather formation. Although the disrupted enhancer segment was critical for modulating *Sim1* expression, its deletion did not impair feather development, suggesting an indirect role for *Sim1* in this process, which warrants further evaluation. Additional studies are also required to clarify the role of *Sim1* in mesenchymal tissues and explore potential compensatory mechanisms. Additionally, as this study focused specifically on flight feather development, the potential functions of *Sim1* in other tissues or processes remain unexplored and should be addressed in future research.

The primary limitation of this study was the partial deletion of the *Sim1*-ASHCE enhancer, with GE chickens retaining approximately 50% of the sequence. Although partial disruption provided valuable insight, complete deletion would be necessary to better elucidate the function of *Sim1*-ASHCE. While PGC-based genome editing is a powerful tool for generating GE chickens, challenges such as maintaining stable culture conditions, achieving high editing efficiency, and the extended timeline required for establishing homozygous GE chickens, remain significant technical obstacles. The Piao PGC line (#P28) was chosen for its robust proliferation, which enabled the efficient identification of donor-derived sperm and offspring through Piao-derived *Fm* and *Rp* mutations. However, delayed secondary flight feather elongation was observed in some G2 individuals, likely due to natural mutations such as sex-linked late feathering (*K*), as reported by Elferink et al. (2008) and Hertwig & Rittershaus (1929), or retarded-tardy feathering (*t*), as reported by Warren (1933), inherited from the donor line. Although normal feather development was eventually achieved, the presence of these mutations complicated the assessment of phenotypic effects resulting from *Sim1*-ASHCE deletion. Establishing a GE chicken line with a genetically uniform background, free of such confounding mutations, will be crucial for accurately evaluating the *Sim1*-ASHCE deletion phenotype. Despite these limitations, this study provides significant insights into the regulatory role of *Sim1*-ASHCE in flight feather development. Partial deletion led to a substantial reduction in *Sim1* expression without impairing flight feather morphology, indicating that compensatory mechanisms likely preserve feather formation in the absence of full *Sim1*-ASHCE activity. Future studies focusing on complete ASHCE deletions and compensatory enhancers will be crucial for clarifying the genetic framework underpinning feather development.

In conclusion, partial deletion of the 284 bp *Sim1*-ASHCE sequence significantly reduced *Sim1* expression but did not produce detectable abnormalities in flight feather development. These findings suggest that flight feather formation can occur with diminished *Sim1* activity, likely supported by compensatory regulatory mechanisms. Delayed feather elongation observed in G2 individuals appears unrelated to *Sim1*-ASHCE deletion and instead reflects natural genetic variation, underscoring the complexity of feather development. Future studies using complete *Sim1*-ASHCE deletion models and exploration of compensatory genes or enhancers will be crucial for fully understanding the role of *Sim1*. These findings also highlight the broader significance of non-coding regulatory elements in evolutionary development and provide a foundation for comparative studies of feather development across diverse avian species.

SUPPLEMENTARY DATA

Supplementary data to this article can be found online.

COMPETING INTERESTS

The authors declare that they have no competing interests.

AUTHORS' CONTRIBUTION

H.J.W. conceived the study. K.K., K.T., T.S., and H.J.W. designed the research; K.K. and K.T. performed the experiments and analyzed the data; K.K., K.T., M.K.S., Y.H.S., and X.Z. contributed reagents/materials/analysis tools/technical support; K.K. wrote the manuscript; H.J.W., T.S., and M.A.J. revised the manuscript and H.J.W., M.A.J., and K.X.X. validated the data. All authors read and approved the final version of the manuscript.

REFERENCES

Ballantyne M, Woodcock M, Doddamani D, et al. 2021. Direct allele introgression into pure chicken breeds using Sire Dam Surrogate (SDS) mating. *Nature Communications*, **12**(1): 659.

Boer EF, Van Hollebeke HF, Shapiro MD. 2017. Genomic determinants of epidermal appendage patterning and structure in domestic birds. *Developmental Biology*, **429**(2): 409–419.

Bonnefond A, Raimondo A, Stutzmann F, et al. 2013. Loss-of-function mutations in *SIM1* contribute to obesity and Prader-Willi-like features. *The Journal of Clinical Investigation*, **123**(7): 3037–3041.

Brown WRA, Hubbard SJ, Tickle C, et al. 2003. The chicken as a model for large-scale analysis of vertebrate gene function. *Nature Reviews Genetics*, **4**(2): 87–98.

Brusatte SL, O'Connor JK, Jarvis ED. 2015. The origin and diversification of birds. *Current Biology*, **25**(19): R888–R898.

Busby L, Aceituno C, McQueen C, et al. 2020. Sonic hedgehog specifies flight feather positional information in avian wings. *Development*, **147**(9): dev188821.

Chen CF, Foley J, Tang PC, et al. 2015. Development, regeneration, and evolution of feathers. *Annual Review of Animal Biosciences*, **3**: 169–195.

Coumailleau P, Duprez D. 2009. *Sim1* and *Sim2* expression during chick and mouse limb development. *The International Journal of Developmental Biology*, **53**(1): 149–157.

Crews ST. 1998. Control of cell lineage-specific development and transcription by bHLH-PAS proteins. *Genes & Development*, **12**(5): 607–620.

Crews ST, Fan CM. 1999. Remembrance of things PAS: regulation of development by bHLH-PAS proteins. *Current Opinion in Genetics & Development*, **9**(5): 580–587.

El-Brolosy MA, Stainier DYR. 2017. Genetic compensation: a phenomenon in search of mechanisms. *PLoS Genetics*, **13**(7): e1006780.

Elferink MG, Vallée AA, Jungerius AP, et al. 2008. Partial duplication of the *PRLR* and *SPEF2* genes at the late feathering locus in chicken. *BMC Genomics*, **9**(1): 391.

Flores-Santin J, Burggren WW. 2021. Beyond the chicken: alternative avian models for developmental physiological research. *Frontiers in Physiology*, **12**: 712633.

Hamburger V, Hamilton HL. 1992. A series of normal stages in the development of the chick embryo. 1951. *Developmental Dynamics*, **195**(4): 231–272.

Hertwig P, Rittershaus T. 1929. Die erbfaktoren der haushühner. *Zeitschrift für Induktive Abstammungs- und Vererbungslehre*, **51**(1): 354–372.

Jarvis ED, Mirarab S, Aberer AJ, et al. 2014. Whole-genome analyses resolve early branches in the tree of life of modern birds. *Science*, **346**(6215): 1320–1331.

Jiang ZQ, Wu HY, Tian J, et al. 2020. Targeting lentiviral vectors to primordial germ cells (PGCs): an efficient strategy for generating transgenic chickens. *Zoological Research*, **41**(3): 281–291.

Kent WJ. 2002. BLAT–the BLAST-like alignment tool. *Genome Research*, **12**(4): 656–664.

Khwatenge CN, Nahashon SN. 2021. Recent advances in the application of CRISPR/Cas9 gene editing system in poultry species. *Frontiers in Genetics*, **12**: 627714.

Kim MJ, Oksenberg N, Hoffmann TJ, et al. 2014. Functional characterization of *SIM1*-associated enhancers. *Human Molecular Genetics*, **23**(7): 1700–1708.

Kinoshita K, Tanabe K, Nakamura Y, et al. 2024. PGC-based cryobanking, regeneration through germline chimera mating, and CRISPR/Cas9-mediated *TYRP1* modification in indigenous Chinese chickens. *Communications Biology*, **7**(1): 1127.

Lamichhaney S, Berglund J, Almén MS, et al. 2015. Evolution of Darwin's finches and their beaks revealed by genome sequencing. *Nature*, **518**(7539): 371–375.

Lee H, Yoon DE, Kim K. 2020. Genome editing methods in animal models. *Animal Cells and Systems*, **24**(1): 8–16.

Lopes RJ, Johnson JD, Toomey MB, et al. 2016. Genetic basis for red coloration in birds. *Current Biology*, **26**(11): 1427–1434.

Lynch M, Mandadzhiev B, Wissa A. 2018. Bioinspired wingtip devices: a pathway to improve aerodynamic performance during low Reynolds number flight. *Bioinspiration & Biomimetics*, **13**(3): 036003.

Metwalli AH, Abellán A, Freixes J, et al. 2022. Distinct subdivisions in the transition between telencephalon and hypothalamus produce Otp and Sim1 Cells for the extended amygdala in sauropsids. *Frontiers in Neuroanatomy*, **16**: 883537.

Michaud JL, Boucher F, Melnyk A, et al. 2001. Sim1 haploinsufficiency causes hyperphagia, obesity and reduction of the paraventricular nucleus of the hypothalamus. *Human Molecular Genetics*, **10**(14): 1465–1473.

Naito Y, Hino K, Bono H, et al. 2015. CRISPRdirect: software for designing CRISPR/Cas guide RNA with reduced off-target sites. *Bioinformatics*, **31**(7): 1120–1123.

Ng CS, Li WH. 2018. Genetic and molecular basis of feather diversity in birds. *Genome Biology and Evolution*, **10**(10): 2572–2586.

Oishi I, Yoshii K, Miyahara D, et al. 2018. Efficient production of human interferon beta in the white of eggs from ovalbumin gene-targeted hens. *Scientific Reports*, **8**(1): 10203.

Osterwalder M, Barozzi I, Tissières V, et al. 2018. Enhancer redundancy provides phenotypic robustness in mammalian development. *Nature*, **554**(7691): 239–243.

Park TS, Lee HJ, Kim KH, et al. 2014. Targeted gene knockout in chickens mediated by TALENs. *Proceedings of the National Academy of Sciences of the United States of America*, **111**(35): 12716–12721.

Perry MM. 1988. A complete culture system for the chick embryo. *Nature*, **331**(6151): 70–72.

Popova J, Bets V, Kozhevnikova E. 2023. Perspectives in genome-editing techniques for livestock. *Animals*, **13**(16): 2580.

Rayner JMV. 1988. Form and function in avian flight. *In*: Johnston RF. Current Ornithology. Boston: Springer, 1–66.

Sackton TB, Grayson P, Cloutier A, et al. 2019. Convergent regulatory evolution and loss of flight in paleognathous birds. *Science*, **364**(6435): 74–78.

Schmittgen TD, Livak KJ. 2008. Analyzing real-time PCR data by the comparative C_T method. *Nature Protocols*, **3**(6): 1101–1108.

Seki R, Li C, Fang Q, et al. 2017. Functional roles of Aves class-specific *cis*-regulatory elements on macroevolution of bird-specific features. *Nature Communications*, **8**(1): 14229.

Terrill RS, Shultz AJ. 2023. Feather function and the evolution of birds. *Biological Reviews*, **98**(2): 540–566.

Warren DC. 1933. Retarded feathering in the fowl: a new factor affecting manner of feathering. *Journal of Heredity*, **24**(11): 431–434.

Whyte J, Glover JD, Woodcock M, et al. 2015. FGF, insulin, and SMAD signaling cooperate for avian primordial germ cell self-renewal. *Stem Cell Reports*, **5**(6): 1171–1182.

Wu P, Yan J, Lai YC, et al. 2018. Multiple regulatory modules are required for scale-to-feather conversion. *Molecular Biology and Evolution*, **35**(2): 417–430.

Xu X, Zhou ZH, Wang XL, et al. 2003. Four-winged dinosaurs from China. *Nature*, **421**(6921): 335–340.